ARL-TN-0982 ● Nov 2019

DEVCOM ARMY RESEARCH LABORATORY

Addendum to ARL-TR-8489, "Morphological and Mechanical Characterization of Adolescent Yucatan Miniature Porcine Skull"

by Stephen L Alexander and Tusit Weerasooriya

NOTICES

Disclaimers

ARL-TN-0982 ● NOV 2019

Addendum to ARL-TR-8489, "Morphological and Mechanical Characterization of Adolescent Yucatan Miniature Porcine Skull"

by Stephen L Alexander
SURVICE Engineering Company

Tusit Weerasooriya
Weapons and Materials Research Directorate, CCDC Army Research Laboratory

REPORT DOCUMENTATION PAGE	*Form Approved* *OMB No. 0704-0188*

1. REPORT DATE *(DD-MM-YYYY)*	**2. REPORT TYPE**	**3. DATES COVERED (From - To)**
November 2019	Technical Note	June 2017–June 2018

4. TITLE AND SUBTITLE
Addendum to ARL-TR-8489, "Morphological and Mechanical Characterization of Adolescent Yucatan Miniature Porcine Skull"

5a. CONTRACT NUMBER
W911QX-16-D-0014

5b. GRANT NUMBER

5c. PROGRAM ELEMENT NUMBER

6. AUTHOR(S)
Stephen L Alexander and Tusit Weerasooriya

5d. PROJECT NUMBER

5e. TASK NUMBER

5f. WORK UNIT NUMBER

7. PERFORMING ORGANIZATION NAME(S) AND ADDRESS(ES)
CCDC Army Research Laboratory
ATTN: FCDD-RLW-PB
Aberdeen Proving Ground, MD 21005-5066

8. PERFORMING ORGANIZATION REPORT NUMBER
ARL-TN-0982

9. SPONSORING/MONITORING AGENCY NAME(S) AND ADDRESS(ES)

10. SPONSOR/MONITOR'S ACRONYM(S)

11. SPONSOR/MONITOR'S REPORT NUMBER(S)

12. DISTRIBUTION/AVAILABILITY STATEMENT
Approved for public release; distribution is unlimited.

13. SUPPLEMENTARY NOTES
As of 31 January 2019, the organization is now part of the US Army Combat Capabilities Development Command (formerly RDECOM) and is now called CCDC Army Research Laboratory.

14. ABSTRACT
Based on the findings of ARL-TR-8489, this addendum presents a simplified mechanical model to describe the structural stress-strain response of the skull of the adolescent Yucatan miniature pig under compression. In particular, ARL-TR-8489 focused only on the initial linear response before the bone microstructure began to fail locally, observed as crushing at the macrostructural scale. The experimental setup was not designed to accurately record the local and global stress-strain response after the bone began to crush and compact. However, a complete stress-strain response up to macroscopic failure, which included both the initial and post-compaction regimes, was needed in order to directly input into finite element simulations involving this species. To our knowledge, such information on the progress of local failure leading to corresponding global response is not currently in the open literature. The mechanical response after initiation of localized failure from other types of bones could not be used without a loss of accuracy in the predictions from simulations due to the large amount of biovariability in bone microstructure and mechanics.

In ARL-TR-8489, the microstructure of the Yucatan skull bone was reported as approximately isotropic at the macro-scale, with low variations of bone volume fraction in the skull. Therefore, in the present addendum, the Yucatan skull is treated as a single homogeneous layer, and its stress-strain response modeled as tri-linear. The initial response is followed by softening while the bone is being crushed. After the bone has fully compacted, the skull stiffness increases considerably until failure.

15. SUBJECT TERMS
Yucatan miniature porcine, skull morphology, mechanical characterization, digital image correlation, micro-X-ray tomography

16. SECURITY CLASSIFICATION OF:			**17. LIMITATION OF ABSTRACT**	**18. NUMBER OF PAGES**	**19a. NAME OF RESPONSIBLE PERSON**
a. REPORT	**b. ABSTRACT**	**c. THIS PAGE**			Stephen L Alexander
					19b. TELEPHONE NUMBER (Include area code)
Unclassified	Unclassified	Unclassified	UU	13	(410) 306-0917

Standard Form 298 (Rev. 8/98)
Prescribed by ANSI Std. Z39.18

Contents

List of Figures

Preface

Based on the findings of ARL-TR-8489,[1] this addendum presents a simplified mechanical model to describe the structural stress-strain response of the skull of the adolescent Yucatan miniature pig under compression. In particular, ARL-TR-8489 focused only on the initial linear response before the bone microstructure began to fail locally, observed as crushing at the macrostructural scale. The experimental setup was not designed to accurately record the local and global stress-strain response after the bone began to crush and compact. However, a complete stress-strain response up to macroscopic failure, which included both the initial and post-compaction regimes, was needed in order to directly input into finite element simulations involving this species. To our knowledge, such information on the progress of local failure leading to corresponding global response is not currently in the open literature. The mechanical response after initiation of localized failure from other types of bones could not be used without a loss of accuracy in the predictions from simulations due to the large amount of biovariability in bone microstructure and mechanics.

In ARL-TR-8489, the microstructure of the Yucatan skull bone was reported as approximately isotropic at the macro-scale, with low variations of bone volume fraction in the skull. Therefore, in the present addendum, the Yucatan skull is treated as a single homogeneous layer, and its stress-strain response modeled as tri-linear. The initial response is followed by softening while the bone is being crushed. After the bone has fully compacted, the skull stiffness increases considerably until failure.

[1] Gunnarsson CA, Alexander SL, Weerasooriya T. Morphological and mechanical characterization of adolescent Yucatan miniature porcine skull. Aberdeen Proving Ground (MD): Army Research Laboratory (US); 2018 Sep. Report No.: ARL-TR-8489.

1. Simplified Deformation/Failure Model for Yucatan miniPig Skull under Compression at Quasi-static Rates

In this addendum, the simplified layered model is based on, and is compared to, the data from the specimen labeled in ARL-TR-8489[1] as 16-02. The engineering stress measured from the experiment is plotted in Fig. 1 as a function of the engineering strain. The strain was calculated from the digital image correlation (DIC)-derived displacement fields on the left and right cameras and by averaging between the two cameras at each time point. The analytical model (assuming layered configuration) was constructed in three parts. In the first part, the modulus of each layer (in this case the single layer) was calculated using the power law relationship between the modulus (E) and bone volume fraction (f_{bv}) previously published at the Army Research Laboratory for Yucatan cranial bone:

$$E = 10990(f_{bv})^{2.6}\text{MPa [ARL-TR-8489]}. \quad (1)$$

The average f_{bv} for Specimen 16-02 was 0.504. The local failure stress, σ^f, was described by an analogous power relationship. This relationship scaled σ_0^f, which is the local failure stress of compacted bone such that $f_{bv} = 1$, by the bone volume fraction:

$$\sigma^f = \sigma_0^f (f_{bv})^k. \quad (2)$$

Here, the exponential scaling parameter, k, was specified as $k = 2$ in keeping with previous publications.[2,3] The parameter σ_0^f was identified as $\sigma_0^f = 85$ MPa by matching to the experimental stress-strain response and indicates that the specimen, after accumulation of debris from compaction, is expected to fail at 85 MPa.

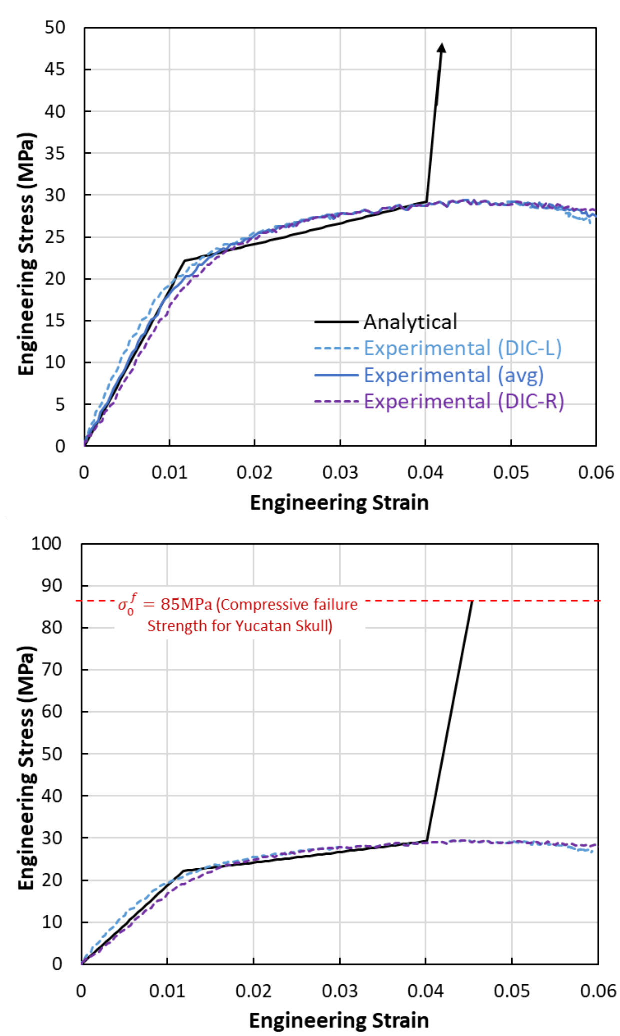

Fig. 1 The engineering stress-strain response from the experiment and analytical model for the initial response (top) and to failure (bottom). Experimental strain was measured from the DIC-derived displacement fields from the left camera (DIC-L), right camera (DIC-R), and as an average between these two cameras at each time point (avg).

The analytical model can be described by the following, using engineering stress and engineering strain:

$$\sigma\ (\text{MPa}) = \begin{cases} 1878.2\varepsilon - 0.1, & (0,0) \le (\sigma, \varepsilon) < (22.1\ \text{MPa}, 0.0118) \\ 250.0\varepsilon + 19.2, & (22.1\ \text{MPa}, 0.0118) \le (\sigma, \varepsilon) < (29.2\ \text{MPa}, 0.0401). \\ 10990\varepsilon - 411.8\,, & (29.2\ \text{MPa}, 0.0401) \le (\sigma, \varepsilon) < (85.0\ \text{MPa}, 0.0452) \end{cases} \quad (3)$$

Note that the model describes the stress response to 85 MPa (ε=0.0452), after which the specimen is predicted to fail under compression (plane stress). The three different regimes of this model are shown in Fig. 2 and in comparison to the experimental stress-strain response.

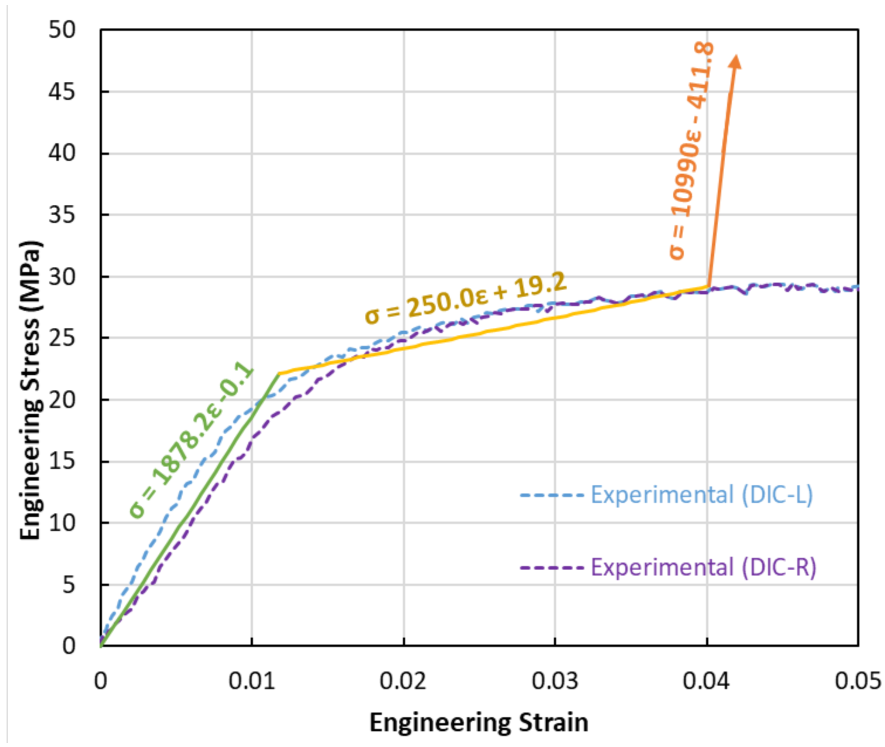

Fig. 2 The engineering stress-strain response in the small-scale regime, with the tri-linear model plotted with the experimental stress-strain curve (as in Fig. 1)

2. References

1. Gunnarsson CA, Alexander SL, Weerasooriya T. Morphological and mechanical characterization of adolescent Yucatan miniature porcine skull. Aberdeen Proving Ground (MD): Army Research Laboratory (US); 2018 Sep. Report No.: ARL-TR-8489.

2. Gibson LJ, Ashby MF. Cellular solids: structure and properties. Cambridge (UK): Cambridge University Press; 1997.

3. Morgan EF, Unnikrisnan GU, Hussein AI. Bone mechanical properties in healthy and diseased states. Annu Rev Biomed Eng. 2018 June 4;20:119–143.

1 DEFENSE TECHNICAL
(PDF) INFORMATION CTR
DTIC OCA

1 CCDC ARL
(PDF) FCDD RLD CL
TECH LIB

12 CCDC SOLDIER CTR
(PDF) M G CARBONI
D COLANTO
R DILLALLA
B FASEL
J FONTECCHIO
B KIMBALL
J KIREJCZYK
J PARKER
M MAFFEO
M MARKEY
D PHELPS
J WARD

2 PROG EXECUTIVE OFC
(PDF) SOLDIER
A FOURNIER
J MULLENIX

1 LAWRENCE BERKELY
(PDF) NATL LAB
R RITCHIE

5 SOUTHWEST RSRCH INST
(PDF) C ANDERSON JR
S CHOCRON
D NICOLELLA
T HOLMQUIST
G JOHNSON

1 INST FOR DEFNS ANLYS
(PDF) Y MACHERET

4 MRMC DOD BLAST INJURY
(PDF) RSRCH PROGRAM COOR OFC
R GUPTA
M LEGGIERI
T PIEHLER
R SHOGE

2 MRMC JTAPIC PRGM OFC
(PDF) W LEI
J USCILOWICZ

1 CCDC GROUND VEHICLE
(PDF) SYS CTR
R SCHERER

4 US ARMY AEROMEDICAL
(PDF) RSRCH LAB
F BROZOSKI
V CHANCEY
B MCENTYRE
D WISE

1 CCDC HQ
(PDF) D RUSIN

2 CCDC CHEM BIO CTR
(PDF) M HORSMON
N VINCELLI

1 OSD DOT&E
(PDF) J IVANCIK

5 US NAVAL RSRCH LAB
(PDF) A BAGCHI
A ILIOPOULOS
J MICHOPOULOS
K TEFERRA
X TAN

5 CCDC DAC
(PDF) FCDD DAD
P BAKER
FCDD DAS LBW
G DIETRICH
FCDD DAS LBE
J GURGANUS
W MERMAGEN
S SNEAD

81 CCDC ARL
(PDF) FCDD RLD P
S WALSH
FCDD RLW
A RAWLETT
S KARNA
S SCHOENFELD
FCDD RLW B
C HOPPEL
FCDD RLW LF
G BROWN
FCDD RLW LH
T EHLERS
L MAGNESS
C MEYER
J NEWILL
D SCHEFFLER
B SCHUSTER
FCDD RLW LL
W OBERLE
FCDD RLW
J BEATTY

J MCCAULEY
J SINGH
M VANLANDINGHAM
FCDD RLW MA
D O'BRIEN
T PLAISTED
K STRAWHECKER
E WETZEL
C YEN
FCDD RLW MB
G GAZONAS
D GRAY
B LOVE
P MOY
J SIETINS
T WALTER
FCDD RLW MC
A BUJANDA
R JENSEN
J LA SCALA
FCDD RLW MD
J SOUTH
R CARTER
B CHEESEMAN
E CHIN
FCDD RLW ME
G GILDE
J LASALVIA
P PATEL
J SWAB
L VARGAS-GONZALEZ
FCDD RLW MF
B DOWDING
S GRENDAHL
FCDD RLW MG
J LENHART
K MASSER
R MROZEK
FCDD RLW PA
S BILYK
FCDD RLW PB
S ALEXANDER
T BAUMER
A BROWN
A DAGRO
B FAGAN
A GOERTZ
A GUNNARSSON
C HAMPTON
M KLEINBERGER
E MATHEIS
J MCDONALD
P MCKEE
K RAFAELS
S SATAPATHY
M SCHEIDLER
M TEGTMEYER
K THOMPSON
T WEERASOORIYA
S WOZNIAK
T ZHANG
FCDD RLW PC
R BECKER
J BRADLEY
D CASEM
C MEREDITH
FCDD RLW PD
R DONEY
B SCOTT
C RANDOW
FCDD RLW PE
M BURKINS
P GILLICH
M LOVE
P SWOBODA
FCDD RLW PF
N GNIAZDOWSKI
R GUPTA
Y HUANG

3 (PDF) JOHNS HOPKINS UNIV
T D NGUYEN
B NOTGHI
S BAILOOR

1 (PDF) GEORGIA INST OF TECH
S MARGULIES

1 (PDF) VIRGINIA POLYTECHNIC
R BATRA

2 (PDF) MASSACHUSETTS INST OF TECHLGY
R RADOVITZKY
S SOCRATE

1 (PDF) PENN STATE UNIV
R KRAFT

1 (PDF) INDIAN INST OF TECH
R BHARDWAJ

1 (PDF) UNIV OF VIRGINIA
R SALZAR